

Functional Rescue of Dystrophin-deficient *mdx* Mice by a Chimeric Peptide-PMO

HaiFang Yin^{1,2}, Hong M Moulton³, Corinne Betts², Thomas Merritt², Yiqi Seow², Shirin Ashraf², QingSong Wang¹, Jordan Boutilier⁴, and Matthew JA Wood²

¹Tianjin–Oxford Joint Laboratory of Gene Therapy, Tianjin Research Centre of Basic Medical Science, Tianjin Medical University, Tianjin, China;

²Department of Physiology, Anatomy and Genetics, University of Oxford, Oxford, UK; ³Biomedical Sciences, College of Veterinary Medicine, Oregon State University, Corvallis, Oregon, USA; ⁴Siga, Corvallis, Oregon, USA

Splice modulation using antisense oligonucleotides (AOs) has been shown to yield targeted exon exclusion to restore the open reading frame and generate truncated but partially functional dystrophin protein. This has been successfully demonstrated in dystrophin-deficient *mdx* mice and in Duchenne muscular dystrophy (DMD) patients. However, DMD is a systemic disease; successful therapeutic exploitation of this approach will therefore depend on effective systemic delivery of AOs to all affected tissues. We have previously shown the potential of a muscle-specific/arginine-rich chimeric peptide-phosphorodiamidate morpholino (PMO) conjugate, but its long-term activity, optimized dosing regimen, capacity for functional correction and safety profile remain to be established. Here, we report the results of this chimeric peptide-PMO conjugate in the *mdx* mouse using low doses (3 and 6 mg/kg) administered via a 6 biweekly systemic intravenous injection protocol. We show 100% dystrophin-positive fibers and near complete correction of the dystrophin transcript defect in all peripheral muscle groups, with restoration of 50% dystrophin protein over 12 weeks, leading to correction of the DMD pathological phenotype and restoration of muscle function in the absence of detectable toxicity or immune response. Chimeric muscle-specific/cell-penetrating peptides therefore represent highly promising agents for systemic delivery of splice-correcting PMO oligomers for DMD therapy.

Received 24 May 2010; accepted 17 June 2010; published online 10 August 2010. doi:10.1038/mt.2010.151

INTRODUCTION

Duchenne muscular dystrophy (DMD) is a severe muscle degenerative disorder resulting from loss-of-function mutations in the *DMD* gene that lead to disruption of the open reading frame and the absence of functional dystrophin protein.¹ Splice modulation using antisense oligonucleotides (AOs) offers a potential therapy for DMD by permitting targeted exon exclusion in the *DMD* pre-mRNA to restore the open reading frame in mutant

DMD transcripts.^{2–13} This results in the production of truncated but partially functional dystrophin isoforms that retain the critical domains.^{14,15} The therapeutic potential of this method has been successfully shown in human subjects following local intramuscular AO injection.^{9,16}

Given that DMD is a systemic disease affecting all peripheral skeletal muscles, successful AO-mediated splice-correction therapy will be critically dependent on effective systemic AO delivery to all affected tissues. Systemic delivery of both 2'-O-methyl phosphorothioate and phosphorodiamidate morpholino (PMO) AOs has been shown to restore dystrophin protein expression in multiple peripheral muscles in dystrophin-deficient *mdx* mice but with low efficiency.^{5,7,17} Recently several groups have shown that the systemic delivery of neutrally charged PMO AOs can be significantly enhanced by direct PMO conjugation to positively charged, arginine-rich, cell-penetrating peptides.^{12,18–20} All studies reported significant body-wide dystrophin protein restoration in multiple muscle groups at lower peptide-PMO conjugate doses, with some limited correction in cardiac muscle, and with amelioration of the *mdx* dystrophic phenotype.

These studies have highlighted the potential of peptide-PMO conjugates as therapeutic agents for DMD. However, they have yet to explore the full range of peptide design space or methods for specific peptide targeting of muscle and heart. We have recently reported the potential of a new class of chimeric peptides incorporating a muscle-specific domain between the arginine-rich cell-penetrating peptide domain and PMO sequence, the prototype being B-MSP-PMO.²¹ This chimeric peptide incorporated the arginine-rich B peptide^{12,18} fused to a muscle-specific heptapeptide (MSP).²² The activity of this peptide-PMO conjugate was critically dependent on design of the chimeric peptide (B-MSP was highly effective whereas MSP-B was not) and offered enhanced dystrophin splice correction over the corresponding B-PMO conjugate lacking the MSP domain. To fully explore the potential of such novel chimeric peptide-PMOs as candidate therapeutic agents for DMD, a series of important questions need to be addressed including; the establishment of an optimal dosing regimen, the long-term or cumulative effects of repeated peptide-PMO delivery on the restoration of dystrophin protein and function, and any possible toxicity/immune response elicited by the chimeric peptide. Here,

Correspondence: HaiFang Yin, Tianjin Research Centre of Basic Medical Science, Tianjin Medical University, Heping District, Tianjin, 300070, China. E-mail: haifangyin@gmail.com or Matthew JA Wood, Department of Physiology, Anatomy and Genetics, University of Oxford, South Parks Road, Oxford, OX1 3QX, UK. E-mail: matthew.wood@dpag.ox.ac.uk

we report the results in which a very low dose, multi-injection regimen provided near complete systemic dystrophin correction and phenotypic reversal in dystrophin-deficient *mdx* mice in the absence of detectable toxicity or immune response.

RESULTS

B-MSP-PMO provides cumulative correction of the *mdx* mouse phenotype at low dose

Previously, we have demonstrated that multiple doses as low as 3 mg/kg could induce successful exon skipping and the detection of large numbers of dystrophin-positive fibers in body-wide muscles in *mdx* mice, albeit with relatively low overall levels of dystrophin protein.²¹ However, the literature suggests that dystrophin has a long half-life of ~6 months,^{23,24} and we therefore reasoned that it might be possible to establish an effective treatment regimen with repeated, multiple low-dose administrations. To test the ability of the B-MSP-PMO AO to provide cumulative molecular correction in the *mdx* mouse, we began using 3-mg/kg dose

injections, comparing single with multiple intravenous 3 mg/kg doses administered biweekly over the course of 12 weeks. One week following the final injection tissue samples from multiple skeletal muscles and the heart were harvested for protein and RNA analysis. Overall, greater levels of dystrophin expression were detected in the multidose-treated animals (Figure 1a). A remarkable difference was observed in the number of dystrophin-positive fibers detected in biceps, triceps, and quadriceps between the multiple- and single-dose injections, with up to 74.6, 21.8, and 33.8% positive myofibers in multi-injection versus 18.3, 1.7, and 6% following single injections, as determined by immunohistochemical staining (Figure 1b). This analysis showed that dystrophin correction was variable between muscle groups, with significantly improved correction in most but not all groups. These findings were corroborated at the RNA level, where reverse transcriptase (RT)-PCR analysis showed enhanced but incomplete splice correction with 3 mg/kg multi-injections compared with single injections (Figure 1c). Western blot data was also consistent with

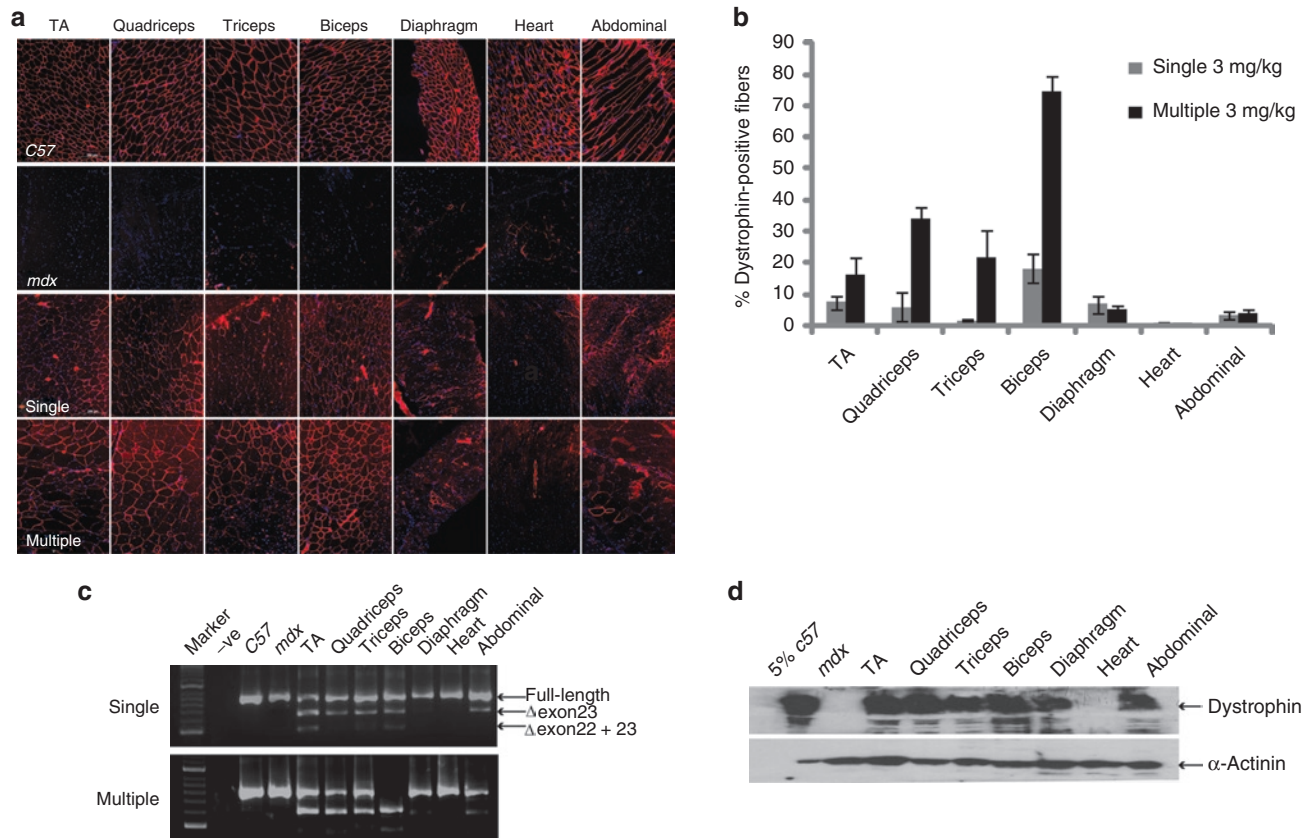


Figure 1 Systemic administration of B-MSP-PMO conjugate at single and multiple 3 mg/kg doses in *mdx* mice. Dystrophin expression following single and six biweekly multiple 3 mg/kg injections of the B-MSP-PMO conjugate in adult *mdx* mice. **(a)** Immunostaining of muscle tissue cross-sections to detect dystrophin protein expression and localization in *mdx* mice treated with single injection (the third panel, single) and multiple injections of B-MSP-PMO conjugates (bottom panel, multiple). Data from control normal *C57BL6* and untreated *mdx* mice were shown (first and the second panel, respectively). Muscle tissues analyzed were from tibialis anterior (TA), quadriceps, triceps, biceps, abdominal wall (abdominal), and diaphragm and heart muscles. Bar = 200 μ m. **(b)** Percent of dystrophin-positive fibers in analyzed muscle tissue cross-sections from *mdx* mice treated with single and multiple 3 mg/kg B-MSP-PMO conjugate doses (six sections per tissue/muscle analyzed). **(c)** RT-PCR analysis to detect dystrophin exon-skipping transcripts in the treated tissues with B-MSP-PMO. Unskipped and skipped transcript products as indicated (exon-skipped bands indicated by Δ exon23—for exon 23 deleted; Δ exon22 + 23—for exons 22 and 23 deleted). **(d)** Western blot for detecting the level of dystrophin protein restored in the analyzed tissues from *mdx* mice treated with multiple 3 mg/kg B-MSP-PMO conjugate doses compared with *C57BL6* and untreated *mdx* control mice. 50 μ g protein was loaded for each sample except for *C57BL6* control lane where 2.5 μ g of protein was loaded. α -Actinin was used as a loading control (six mice in each group). MSP, muscle-specific heptapeptide; PMO, phosphorodiamidate morpholino; RT, reverse transcriptase.

these findings showing restored dystrophin protein in all muscles including diaphragm, but with the exception of heart (Figure 1d). However, the levels of detectable dystrophin protein were not >5% of wild-type *C57BL6* mouse normal levels in the multi-injection group, with less protein detectable following single injections (data not shown). Despite these relatively low levels of dystrophin correction following the multidose 3 mg/kg injection protocol, lower serum creatinine kinase (CK) and serum aspartate aminotransferase enzymes were detected (Supplementary Figure S1a,b), indicative of a degree of correction of the muscle pathology. In addition, grip strength tests showed significant improvement in muscle function in the treated *mdx* mice compared with untreated *mdx* controls (Supplementary Figure S1c).

Cumulative, enhanced molecular and phenotypic correction of *mdx* mice following intravenous 6 mg/kg multidose B-MSP-PMO injections

The data above showed that a multidose regimen for intravenous B-MSP-PMO administration was promising and could lead to appreciable cumulative dystrophin correction in *mdx* mice. We

hypothesized that a critical dose threshold was probably required in order to induce effective dystrophin correction and therefore investigated a higher dose, multi-injection protocol. Using an intravenous dose of 6 mg/kg of B-MSP-PMO administered biweekly over the course of 12 weeks, we found virtually complete dystrophin splice correction at the RNA level in all examined muscles, with the exception of heart. Multidose compared with single 6 mg/kg B-MSP-PMO injections resulted in significant correction of dystrophin expression levels in multiple peripheral muscle groups (Figure 2a). Hundred percentage of myofibers were dystrophin-positive in all muscle groups except heart treated with multiple 6 mg/kg B-MSP-PMO injections, suggesting that a cumulative effect was established following multidose treatment at the higher dose (Figure 2b). This was corroborated by the RT-PCR analysis, which showed the absence of uncorrected dystrophin transcript in all tissues analyzed except heart and abdominal muscle (Figure 2c), indicating complete removal of the mutated exon 23 from the defective *DMD* transcript. This led to increased absolute levels of dystrophin protein as determined by western blot with up to 60% of normal dystrophin protein

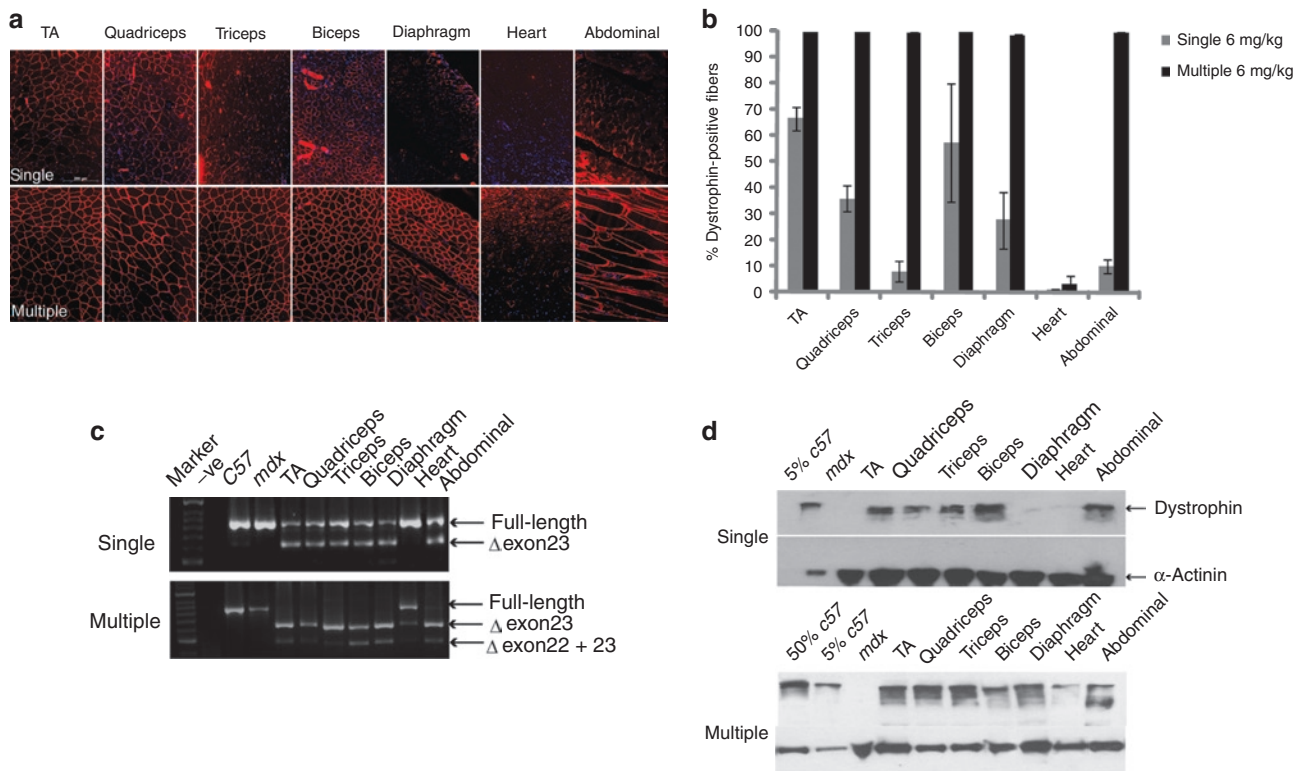


Figure 2 Long-term study of B-MSP-PMO conjugate at the dose of 6 mg/kg following six biweekly injections in *mdx* mice. Dystrophin exon skipping and protein expression following single and multiple systemic doses of the B-MSP-PMO conjugate in adult *mdx* mice. **(a)** Immunohistochemistry to detect dystrophin expression in muscle cross-sections from *mdx* mice treated with B-MSP-PMO at single 6 mg/kg dose (upper panel, single) and multiple 6 mg/kg injections (lower panel, multiple). Data from control normal *C57BL6* and untreated *mdx* mice not shown. Muscle tissues analyzed were from tibialis anterior (TA), quadriceps, triceps, biceps, abdominal wall (abdominal), diaphragm and heart muscles. Bar = 200 μm. **(b)** Percent of dystrophin-positive fibers in the analyzed tissues from treated *mdx* mice. Results show 100% dystrophin-positive fibers observed in all the indicated muscles except heart (six sections per tissue/muscle analyzed). **(c)** RT-PCR to detect the dystrophin exon-skipping products in treated *mdx* mouse muscle groups as shown (exon-skipped bands indicated by Δexon23—for exon 23 deleted; Δexon22 + 23—for exons 22 and 23 deleted). **(d)** Western blot for detection of dystrophin protein in the indicated muscle groups from treated *mdx* mice compared with *C57BL6* and untreated *mdx* control mice. Top panel is for single injection and the bottom one represents multiple injections. Twenty-five microgram protein was loaded for each sample except for *C57BL6* control lane where a corresponding amount of protein was loaded for different treatments as indicated. α-Actinin was used as the loading control (six mice in each group). MSP, muscle-specific heptapeptide; PMO, phosphorodiamidate morpholino; RT, reverse transcriptase.

levels detectable in quadriceps and triceps as measured by Image J software analysis (Figure 2d).

Unsurprisingly, such effective dystrophin splice correction at the molecular level led to phenotypic recovery of treated *mdx* mice. This was shown by functional improvement of the treated *mdx* mouse muscle as shown by grip strength analysis (Figure 3a).^{25,26} In addition, molecular correction was reflected in terms of single-muscle fiber resistance to damage as demonstrated by physiological analysis of isolated extensor digitorum longus muscles, which showed increased maximum force and decreased percent force drop in multidose 6 mg/kg treated mice compared with age-matched *mdx* controls (Supplementary Figure S2). The percentage of muscle fibers with centrally located nuclei is an index of ongoing degeneration/regeneration cycles.^{27,28} Counts of centrally located nuclei within treated *mdx* muscle groups (tibialis anterior, biceps, and quadriceps) revealed a significant reduction in centrally nucleated myofibers compared with untreated control *mdx* mice, suggesting a reduced regenerative stimulus commensurate with improved function (Figure 3b). A significant decline in serum CK levels was also observed in mice

treated with multiple 6 mg/kg doses compared with untreated *mdx* mice (Figure 3c).²⁷ Dystrophin is an essential component of a sarcolemmal dystrophin-associated protein complex (DAPC), which has important signaling functions via neuronal nitric oxide synthase and other molecular components.²⁹ In the absence of functional dystrophin, DAPC components fail to localize accurately to the sarcolemma. We therefore investigated whether successful relocalization of DAPC components was present after cumulative restoration of dystrophin. Relocalization of multiple DAPC component proteins including β -dystroglycan, α -sarcoglycan, and neuronal nitric oxide synthase, was detected following multidose B-MSP-PMO treatment as shown by serial immunostaining of dystrophin and DAPC components (Figure 3d).

Repeated B-MSP-PMO treatment restores functional dystrophin expression in the absence of detectable toxicity or immune response

The 6 mg/kg multidose injection protocol above led to near complete dystrophin splice correction in multiple muscle groups. Given

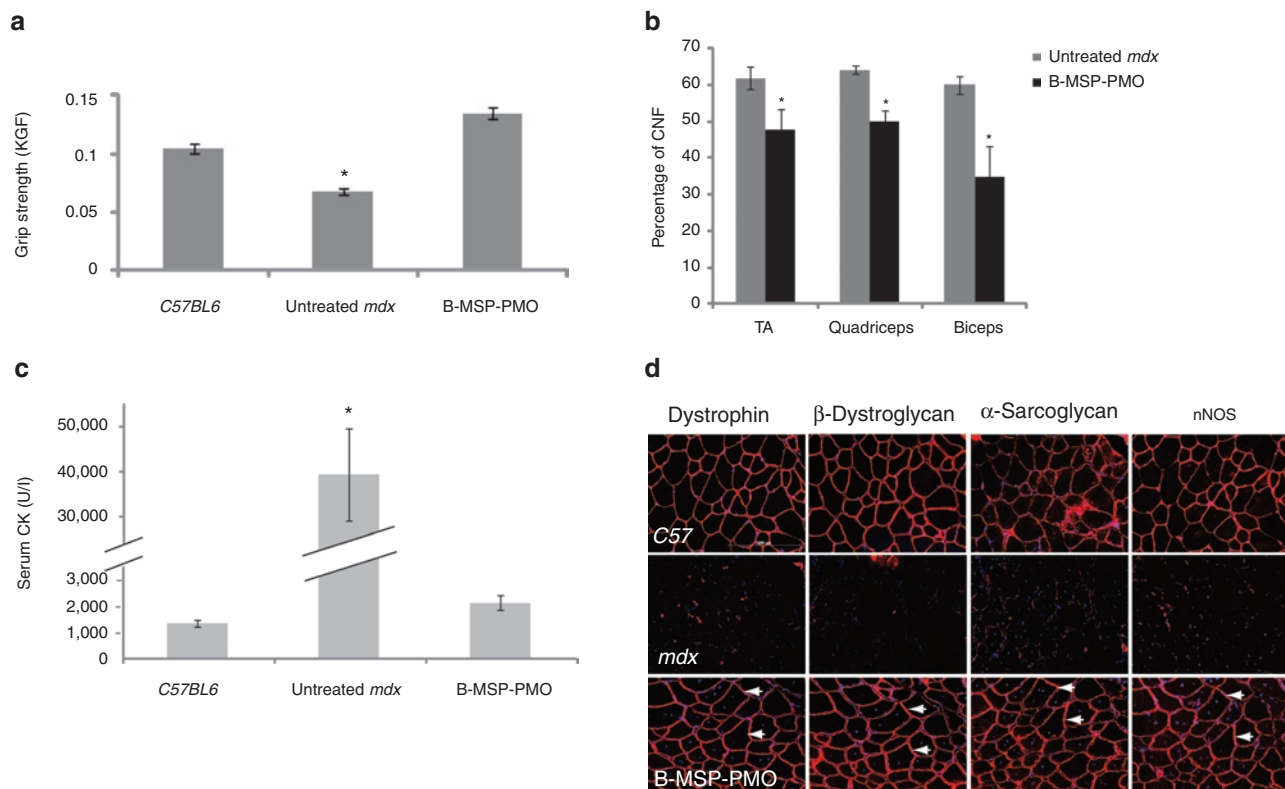


Figure 3 Functional and phenotypic correction in *mdx* mice following treatment with the B-MSP-PMO conjugate at six biweekly 6 mg/kg doses. **(a)** Muscle function was assessed using a functional grip strength test to determine the physical improvement of B-MSP-PMO-treated *mdx* mice. Significant force recovery was detected in treated *mdx* mice compared with untreated controls (*t*-test, $*P < 0.05$; six mice each group). **(b)** Evaluation of the numbers of centrally nucleated myofibers in TA, quadriceps, and biceps muscles following repeated B-MSP-PMO treatment compared with the corresponding untreated *mdx* muscles. Data show a significant decrease in the number of centrally nucleated myofibers in treated *mdx* muscles compared with untreated controls (*t*-test, $P < 0.05$; six sections per tissue/muscle analyzed; six mice each group). **(c)** Measurement of serum creatine kinase (CK) levels as an index of ongoing muscle membrane instability in treated *mdx* mice compared with *mdx* control mice. Data show a significant fall in the serum CK levels in *mdx* mice treated with B-MSP-PMO compared with untreated age-matched *mdx* controls (*t*-test, $P < 0.05$; six mice each group). **(d)** Restoration of the dystrophin-associated protein complex (DAPC) in *mdx* mice with repeated B-MSP-PMO treatment at 6 mg/kg was studied to assess dystrophin function and recovery of normal myoarchitecture. DAPC protein components β -dystroglycan, α -sarcoglycan, and nNOS were detected by immunostaining in serial tissue cross-sections of TA muscles from treated *mdx* mice compared with untreated *mdx* mice and normal C57BL6 mice (arrow indicated identical muscle fibers). Bar = 200 μ m. MSP, muscle-specific heptapeptide; nNOS, neuronal nitric oxide synthase; PMO, phosphorodiamidate morpholino.

this impressive phenotypic correction, we wished to determine whether any side-effects of treatment occurred. We monitored the body weight of *mdx* mice treated with B-MSP-PMO conjugate at 6 mg/kg multidose injections over the course of 12 weeks. Treated mice showed a steady weight increase to the experimental end point as did with untreated age-matched controls (**Supplementary Figure S3**). We also investigated any potential systemic cytotoxicity induced by the repeated treatment with B-MSP-PMO by analyzing serum indexes of liver and kidney damage and function including serum aspartate aminotransferase and alanine aminotransferase liver enzymes levels. The serum levels of these enzymes were reduced to within the normal range compared with untreated *mdx* mice and normal age-matched *C57BL6* control mice (**Figure 4a**). No change was found in the serum levels of urea and creatinine with B-MSP-PMO treatment compared with untreated *mdx* controls and normal mice (data not shown), suggesting no adverse effects of treatment on renal function. We

also undertook histological studies with haematoxylin and eosin staining of liver and kidney tissue sections from *mdx* mice treated with B-MSP-PMO conjugate, which revealed no deleterious changes in tissue morphology or increased numbers of infiltrating cells compared with untreated *mdx* mice (**Figure 4b**). Also there was no increase in the number of other inflammatory infiltrating cells (e.g., macrophage and neutrophil) in muscle sections from *mdx* mice treated with B-MSP-PMO in comparison with untreated controls (**Supplementary Figure S4a**).

Given the striking cumulative effect of dystrophin restoration with multidose of B-MSP-PMO conjugate at 3 and 6 mg/kg, respectively as above, this suggests that B-MSP-PMO is unlikely to induce a significant immune response following repeated administration. This was first tested by immunostaining of CD3⁺ and CD8⁺ T lymphocytes in muscle tissue sections. Sporadic CD3⁺ and CD8⁺ cells were observed in diaphragmatic cross-sections from mice treated with B-MSP-PMO conjugate, however increased numbers were

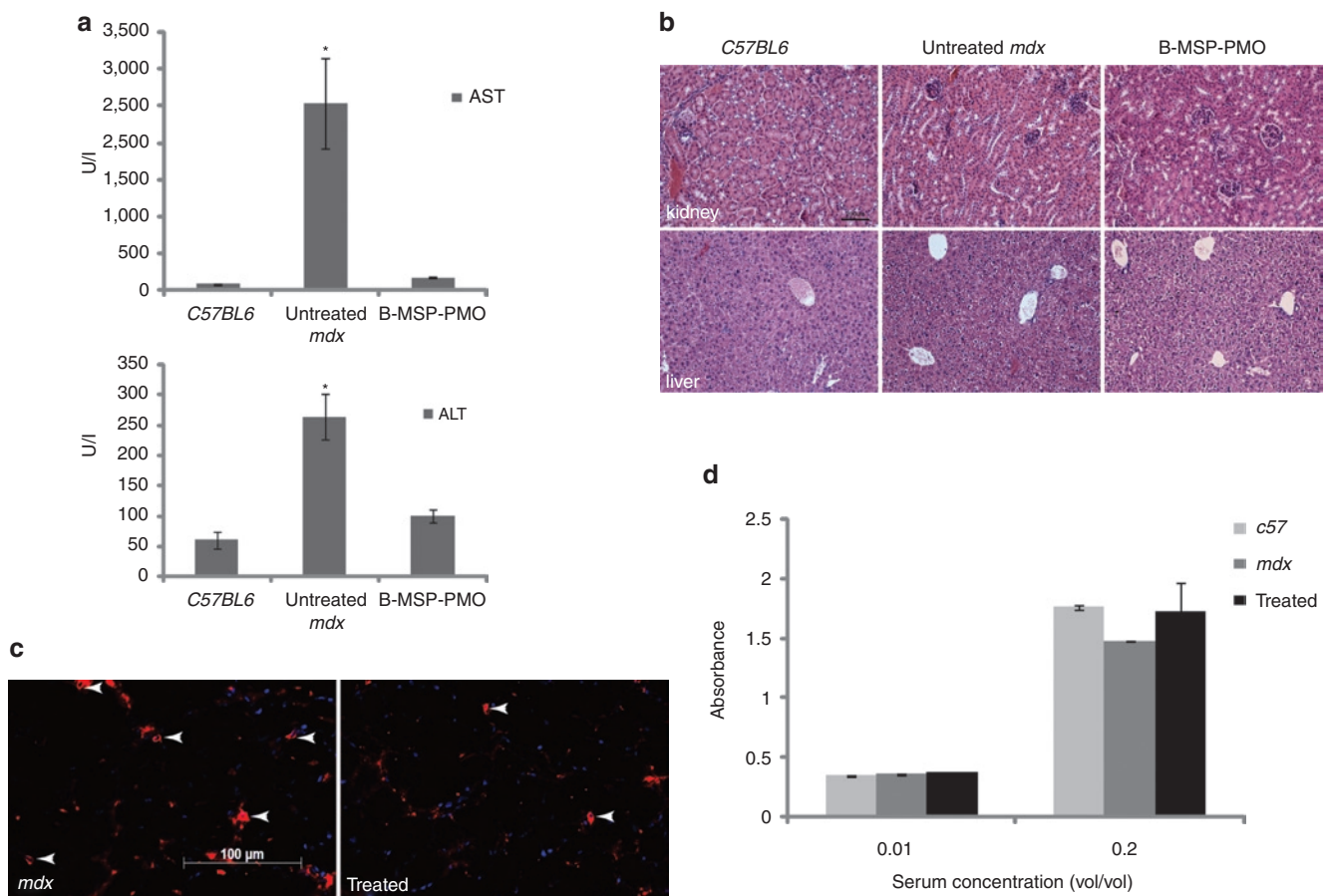


Figure 4 Investigation of systemic immunotoxicity in *mdx* mice treated with the multiple B-MSP-PMO conjugate administration. **(a)** Measurement of serum levels of aspartate aminotransferase (AST) and alanine aminotransferase (ALT) enzymes in treated *mdx* mice compared with untreated *mdx* mice. Data show a improved pathological parameters in B-MSP-PMO-treated *mdx* mice compared with untreated controls with significantly lower serum levels of both enzymes (*t*-test, **P* < 0.05; six mice each group). **(b)** Hematoxylin and eosin staining of kidney (upper panel) and liver (lower panel) tissues sections from treated *mdx* mice with B-MSP-PMO, untreated *mdx* mice, and *C57BL6* normal controls. Bar = 200 μ m. Tissue sections from renal cortex show normal glomerular and tubule tissue architecture in B-MSP-PMO treated and control mice. No difference was observed for B-MSP-PMO treated *mdx* mice and untreated *mdx* controls in liver sections. **(c)** Detection of CD3⁺ T lymphocytes in the diaphragms of treated and untreated *mdx* mice. Bar = 100 μ m. Arrows indicate the T lymphocytes detected by CD3 mouse monoclonal antibody. **(d)** ELISA results to detect specific antibody against the B-MSP-PMO compound in the serum from the treated *mdx* mice at 6 mg/kg biweekly dosing regimens. No difference was observed between treated and untreated *mdx* mice (six mice each group). ELISA, enzyme-linked immunosorbent assay; MSP, muscle-specific heptapeptide; PMO, phosphorodiamidate morpholino.

found in untreated *mdx* controls (Figure 4c; Supplementary Figure S4b), suggesting that B-MSP-PMO lacks immunogenicity. In order to detect any specific humoral immune response in the serum from repeated B-MSP-PMO-treated *mdx* mice, we coated the B-MSP-PMO conjugate on enzyme-linked immunosorbent assay plates as an antigen, and probed with serum collected from B-MSP-PMO-treated *mdx* mice and untreated controls to detect any B-MSP-PMO-specific antibody in serum. Using this assay, only background levels of signal were observed in the treated and untreated controls (Figure 4d), consistent with the functional improvement and phenotypic correction induced in B-MSP-PMO-treated *mdx* mice. Overall, these results indicated that repeated B-MSP-PMO administration failed to elicit any overt toxicity or significant immune response at the dosing regimen utilized.

DISCUSSION

Peptide-conjugated PMO oligomers have significant potential as splice correcting therapeutic agents for DMD.^{12,19,20,30} However, the ability of such agents to incorporate muscle-specific peptides and to provide cumulative molecular and functional correction of the DMD phenotype has not yet been shown. Here, we report studies investigating the therapeutic potential of the novel chimeric peptide-PMO conjugate B-MSP-PMO. We show that while a multi-injection 3 mg/kg intravenous administration regimen was slightly more effective than single injections at this dose in terms of dystrophin restoration, it failed to reach the critical dose threshold required for high-level correction in *mdx* mice. Variation of dystrophin expression between different muscles can be observed with single intravenous injection of B-MSP-PMO (Figure 1b), which indicates that at marginal doses local factors within individual muscle groups might influence AO uptake and/or efficiency. In contrast, a higher dose of 6 mg/kg administered biweekly for 6 weeks resulted in complete molecular correction of the dystrophin defect at the RNA level and in terms of numbers of dystrophin-positive myofibers in multiple peripheral muscle groups including diaphragm. This resulted in cumulative correction of molecular and pathological features associated with the *mdx* phenotype including decreased serum CK levels, restored DAPC localization, improved grip function, and other physiological parameters, in the absence of detectable immune response or toxicity. The mechanism for this improved activity appears to be related to increased muscle cell uptake or internalization of the PMO conjugate as demonstrated by our recent study (data not shown). Chimeric muscle-specific peptides conjugated to PMO AOs therefore have significant potential as therapeutic agents for systemic splice correction in DMD.

Two major questions arise in the use of peptide PMO conjugates for dystrophin restoration. The first is to what extent muscle function is restored and ongoing muscle degenerative pathology is halted or reversed. At the 6 mg/kg, repeat dose the restored dystrophin protein is functional as evidenced by efficient restoration of the dystrophin network of proteins at the sarcolemma (the DAPC) and improved *mdx* muscle grip strength and single-muscle fiber resistance to damage to within the normal range. Multiple indexes of disease pathology including serum CK levels, aspartate aminotransferase/alanine aminotransferase and routine muscle histology all showed significant reversal of disease

progression. Although the percentage of centrally nucleated myofibers in treated samples remained high, there was significant decrease compared with untreated *mdx* controls, which indicated the progression of the disease pathology was significantly altered. The data was corroborated by the absence or low numbers of regenerating fibers and significantly decreased amount of collagen deposition detected in treated samples (Supplementary Figure S4c–e). The second question relates to safety and potential immunotoxicity of the peptide PMO compound. At the multidose regimen used in this study all indexes of organ or immunotoxicity were negative including serum indexes of hepatic and renal function within the normal range, normal liver and kidney histology, no accumulation of infiltrating CD3⁺/CD8⁺T lymphocytes and macrophages/neutrophils within tissues and no evidence by enzyme-linked immunosorbent assay of serum antibodies directed against the B-MSP-PMO conjugate. During the study, the treated *mdx* mice showed the same pattern of weight gain as untreated age-matched controls. Therefore low dose, repeated administration of this B-MSP-PMO compound provides virtually complete correction of dystrophin expression in all peripheral muscle groups and this correlates with functional correction of muscle physiology and reversal of pathological indicators in the absence of detectable immunotoxicity.

The data presented therefore suggest that B-MSP-PMO has significant potential as a therapeutic agent for the long-term treatment of the dystrophin muscle defect in patients with DMD. This work is a prelude to even longer term studies (1–2 years) to ascertain the effects of lifetime correction of dystrophin deficiency in *mdx* mice, and provides strong evidence for the use of such chimeric peptide PMO conjugates as therapeutic agents in DMD patients. That relatively poor dystrophin correction was found in heart is consistent with our previous report identifying this chimeric peptide PMO conjugate,²¹ in which we have shown only a slightly higher level of dystrophin expression in heart with B-MSP-PMO compared with the parent B-PMO compound at a 25 mg/kg dose. Our speculation is that the low level of dystrophin splice correction in heart is most likely due to the high affinity of MSP for skeletal muscle and the low-dose regimen used in this study. Nevertheless, the opportunity now exists to identify different or improved versions of the MSP tissue-specific domain including cardiac-specific peptides, and the study of such conjugated PMOs is already in progress (data not shown).

MATERIALS AND METHODS

Animals. Six to eight-week-old *mdx* mice were used in all experiments (six mice each in the test and control groups). The experiments were carried out in the Animal Unit, Department of Physiology, Anatomy and Genetics (University of Oxford, Oxford, UK) according to procedures authorized by the UK Home Office. Mice were killed by CO₂ inhalation at desired time points, and muscles and other tissues were snap-frozen in liquid nitrogen-cooled isopentane and stored at –80 °C.

PMO and peptide-PMO conjugates. Peptide-conjugated PMOs were synthesized and purified to >90% purity by AVI Biopharma (Corvallis, OR). The nomenclature and sequences of this B-MSP-PMO conjugate is (RXRRBR)₂-ASSLNIAAX-PMO. The PMO AO 5'-ggccaacacctcgcttacctgaat-3' was targeted to the murine dystrophin exon 23/intron 23 boundary site. MSP is a muscle-specific heptapeptide, previously identified by *in vivo* phage

display as having increased muscle- and cardiac-binding properties.²² B peptide is a derivative of a previously described arginine-rich peptide (RXR)₄^{18,30} in which two of the non-natural 6-aminohexanoic acid (X) residues were substituted with non-natural amino acid β-alanine. B-MSP is a chimeric peptide of B and MSP with the MSP positioned at the C-terminus of the B peptide. The PMO was conjugated to the carboxyl groups at the C-terminus of the peptide using a method described elsewhere.^{18,30}

RNA extraction and nested RT-PCR analysis. Total RNA was extracted with Trizol (Invitrogen, Renfrew, UK) and 200 ng of RNA template was used for 20 μl RT-PCR with OneStep RT-PCR kit (Qiagen, West Sussex, UK). The primer sequences and reaction conditions were used as previously reported.^{11,12} The first step RT-PCR was carried out with the OneStep RT-PCR kit with 25 cycles for PCR step and another 25 cycles was applied for the following nested PCR. The products were examined by electrophoresis on a 2% agarose gel.

Systemic injections of peptide-PMO conjugates. Various amounts of peptide-PMO conjugate in 80 μl saline buffer were injected into tail vein of *mdx* mice at the final dose of 3 and 6 mg/kg, respectively.

Immunohistochemistry and histology. Series of 8-μm sections were examined for dystrophin expression and DAPC with a series of polyclonal antibodies and monoclonal antibodies as described.¹² CD3⁺/CD8⁺ T lymphocytes cell were identified with rat polyclonal³¹ and mouse monoclonal primary antibody (eBioscience, Hatfield, UK), respectively; then detected by goat-anti-rat and goat-anti-mouse immunoglobulin Gs Alexa 594 (Invitrogen). For macrophage and neutrophil staining, polyclonal rabbit and rat primary antibodies from Abcam (Cambridge, UK) were used, respectively. Collagen IV polyclonal rabbit primary antibody was applied for collagen staining (Abcam) and Image J software analysis was used for quantification. For detecting regenerating muscle fibers, mouse fetal myosin antibody was used, which was a gift from Professor Neal A. Rubinstein (University of Pennsylvania, Philadelphia, PA). Goat-anti-rabbit, -rat and -mouse immunoglobulin Gs Alexa 594 secondary antibodies were applied, respectively (Invitrogen). Routine haematoxylin and eosin staining was used to examine overall liver and kidney morphology.

Enzyme-linked immunosorbent assay for serum antibody detection. An enzyme-linked immunosorbent assay was adopted from a previously published method.¹⁸ The serum from treated and untreated *mdx* mice was collected at the end point. Plates were coated with 1 μg B-MSP-PMO conjugate, incubated at 4 °C overnight, washed, blocked with normal goat serum and incubated with serum from *C57BL6* mice and the treated *mdx* mice in serial dilutions for 1 hour. The plates were then incubated with goat-anti-mouse immunoglobulin G horseradish peroxidase (Sigma, Hertfordshire, UK) for 30 minutes. The substrate was applied for 10–30 minutes and the reaction was terminated by the stop solution from the Substrate Pack (R&D Systems, Minneapolis, MN). The signal intensity was measured by the plate reader (PerkinElmer, Beaconsfield, UK).

Centrally nucleated fiber counts. Tibialis anterior, quadriceps, and triceps muscles from *mdx* mice treated with B-MSP-PMO conjugate were examined. To ascertain the number of centrally nucleated muscle fibers, sections were stained for dystrophin with rabbit polyclonal antibody 2166 and counter-stained with DAPI for cell nuclei (Sigma). 500–1,000 dystrophin-positive fibers for each tissue sample were randomly chosen, counted and assessed for the presence of central nuclei using a Zeiss AxioVision fluorescence microscope (Carl Zeiss, Herts, UK). Fibers were judged centrally nucleated if one or more nuclei were not located at the periphery of the fiber. Untreated age-matched *mdx* mice were used as controls.

Protein extraction and western blot. Protein extraction and western blot were carried out as previously described.¹² Various amounts of protein from normal *C57BL6* mice as a positive control and corresponding

amounts of protein from muscles of treated or untreated *mdx* mice were used. α-Actinin was used as loading control. The intensity of the bands obtained from treated *mdx* muscles was measured by Image J software; the quantification is based on band intensity and area, and is compared with that from normal muscles of *C57BL6* mice.

Functional grip strength and physiological analysis. Treated and control mice were tested using a commercial grip strength monitor (Chatillon, West Sussex, UK). The procedure is the same as previously described.¹² Each mouse was held 2 cm from the base of the tail, allowed to grip a protruding metal triangle bar attached to the apparatus with their fore-paws, and pulled gently until they released their grip. The force exerted was recorded and five sequential tests were carried out for each mouse, averaged at 30 seconds apart. Subsequently the readings for force recovery were normalized by the body weight. For isolated muscle fiber physiological analysis, the extensor digitorum longus muscle was used as reported,³² and contractile properties determined using previous methods.³³ The muscle was subjected to single pulses of 0.2 ms in duration at 30 V whereas the optimum length (L_o) for development of maximum isometric twitch force was determined. Fiber length (L_f) was determined by multiplying the figure obtained for L_o by the predetermined fiber length to muscle length ratio of 0.45.³⁴ The maximum isometric force (P_o) was calculated from the peak of the curve, as was data required to calculate time to half-peak and time to half-relaxation. Eccentric contractions were performed during a 0.75 seconds protocol.³² All data was digitized and analyzed using the DMA software (version 3.2; Aurora Scientific, Bristol, UK).

Clinical biochemistry. Serum and plasma were taken from the mouse jugular vein immediately after the killing with CO₂ inhalation. Analysis of serum CK, aspartate aminotransferase, alanine aminotransferase, urea and creatinine levels was performed by the clinical pathology laboratory (Mary Lyon Centre, Medical Research Council, Harwell, Oxfordshire, UK).

Statistical analysis. All data are reported as mean values ± SEM. Statistical differences between treatment groups and control groups were evaluated by SigmaStat (Systat Software, London, UK) and the Student's *t*-test was applied.

SUPPLEMENTARY MATERIAL

Figure S1. Phenotypic and functional improvement in *mdx* mice treated with 6 biweekly 3 mg/kg B-MSP-PMO conjugate.

Figure S2. Physiological improvement in *mdx* mice treated with B-MSP-PMO conjugate at 6 biweekly 6 mg/kg repeated doses.

Figure S3. Body-weight measurements of *mdx* mice treated with 6 biweekly B-MSP-PMO at 3 and 6 mg/kg doses over 12 weeks.

Figure S4. Investigation of other parameters in *mdx* mice treated with B-MSP-PMO conjugate at 6 biweekly 6 mg/kg repeated doses.

ACKNOWLEDGMENTS

This work was supported by research grants from the UK Department of Health and the UK Muscular Dystrophy Campaign to M.J.A.W. The authors acknowledge the UK MDEX Consortium for helpful discussions; Professor Kay Davies (Department of Physiology, Anatomy and Genetics, University of Oxford, Oxford, UK) for providing access to facilities including the *mdx* mouse colony; Dave Powell (Department of Physiology, Anatomy and Genetics, University of Oxford) for assistance with physiological assays; Dr Hough (Clinical Pathology Laboratory, Mary Lyon Centre, MRC, Harwell, UK) for assistance with the clinical biochemistry assays; Christine Simpson (Department of Physiology, Anatomy and Genetics, University of Oxford) for assistance with histology; and Jed Hissinger (AVI Biopharma Inc., Corvallis, Oregon) for the synthesis of MSP-PMO conjugates. The authors declared no conflict of interest.

REFERENCES

1. Wood, MJ, Gait, MJ and Yin, H (2010). RNA-targeted splice-correction therapy for neuromuscular disease. *Brain* **133**(Pt 4): 957–972.

2. Aartsma-Rus, A, Janson, AA, Kaman, WE, Bremmer-Bout, M, den Dunnen, JT, Baas, F *et al.* (2003). Therapeutic antisense-induced exon skipping in cultured muscle cells from six different DMD patients. *Hum Mol Genet* **12**: 907–914.
3. Aartsma-Rus, A, Janson, AA, Kaman, WE, Bremmer-Bout, M, van Ommen, GJ, den Dunnen, JT *et al.* (2004). Antisense-induced multiexon skipping for Duchenne muscular dystrophy makes more sense. *Am J Hum Genet* **74**: 83–92.
4. Aartsma-Rus, A, Kaman, WE, Weij, R, den Dunnen, JT, van Ommen, GJ and van Deutekom, JC (2006). Exploring the frontiers of therapeutic exon skipping for Duchenne muscular dystrophy by double targeting within one or multiple exons. *Mol Ther* **14**: 401–407.
5. Alter, J, Lou, F, Rabinowitz, A, Yin, H, Rosenfeld, J, Wilton, SD *et al.* (2006). Systemic delivery of morpholino oligonucleotide restores dystrophin expression bodywide and improves dystrophic pathology. *Nat Med* **12**: 175–177.
6. GebSKI, BL, Mann, CJ, Fletcher, S and Wilton, SD (2003). Morpholino antisense oligonucleotide induced dystrophin exon 23 skipping in mdx mouse muscle. *Hum Mol Genet* **12**: 1801–1811.
7. Lu, QL, Mann, CJ, Lou, F, Bou-Gharios, G, Morris, GE, Xue, SA *et al.* (2003). Functional amounts of dystrophin produced by skipping the mutated exon in the mdx dystrophic mouse. *Nat Med* **9**: 1009–1014.
8. Mann, CJ, Honeyman, K, Cheng, AJ, Ly, T, Lloyd, F, Fletcher, S *et al.* (2001). Antisense-induced exon skipping and synthesis of dystrophin in the mdx mouse. *Proc Natl Acad Sci USA* **98**: 42–47.
9. van Deutekom, JC, Janson, AA, Ginjaar, IB, Frankhuizen, WS, Aartsma-Rus, A, Bremmer-Bout, M *et al.* (2007). Local dystrophin restoration with antisense oligonucleotide PRO051. *N Engl J Med* **357**: 2677–2686.
10. Wilton, SD, Fall, AM, Harding, PL, McClorey, G, Coleman, C and Fletcher, S (2007). Antisense oligonucleotide-induced exon skipping across the human dystrophin gene transcript. *Mol Ther* **15**: 1288–1296.
11. Yin, H, Lu, Q and Wood, M (2008). Effective exon skipping and restoration of dystrophin expression by peptide nucleic acid antisense oligonucleotides in mdx mice. *Mol Ther* **16**: 38–45.
12. Yin, H, Moulton, HM, Seow, Y, Boyd, C, Boutilier, J, Iverson, P *et al.* (2008). Cell-penetrating peptide-conjugated antisense oligonucleotides restore systemic muscle and cardiac dystrophin expression and function. *Hum Mol Genet* **17**: 3909–3918.
13. Heemskerck, HA, de Winter, CL, de Kimpe, SJ, van Kuik-Romeijn, P, Heuvelmans, N, Platenburg, CJ *et al.* (2009). *In vivo* comparison of 2'-O-methyl phosphorothioate and morpholino antisense oligonucleotides for Duchenne muscular dystrophy exon skipping. *J Gene Med* **11**: 257–266.
14. England, SB, Nicholson, LV, Johnson, MA, Forrest, SM, Love, DR, Zubrzycka-Gaarn, EE *et al.* (1990). Very mild muscular dystrophy associated with the deletion of 46% of dystrophin. *Nature* **343**: 180–182.
15. Gregorevic, P, Blankinship, MJ and Chamberlain, JS (2004). Viral vectors for gene transfer to striated muscle. *Curr Opin Mol Ther* **6**: 491–498.
16. Kinali, M, Arechavala-Gomez, V, Feng, L, Cirak, S, Hunt, D, Adkin, C *et al.* (2009). Local restoration of dystrophin expression with the morpholino oligomer AVI-4658 in Duchenne muscular dystrophy: a single-blind, placebo-controlled, dose-escalation, proof-of-concept study. *Lancet Neurol* **8**: 918–928.
17. Heemskerck, H, de Winter, C, van Kuik, P, Heuvelmans, N, Sabatelli, P, Rimessi, P *et al.* (2010). Preclinical PK and PD studies on 2'-O-methyl-phosphorothioate RNA antisense oligonucleotides in the mdx mouse model. *Mol Ther* **18**: 1210–1217.
18. Jearawiriyapaisarn, N, Moulton, HM, Buckley, B, Roberts, J, Sazani, P, Fucharoen, S *et al.* (2008). Sustained dystrophin expression induced by peptide-conjugated morpholino oligomers in the muscles of mdx mice. *Mol Ther* **16**: 1624–1629.
19. Wu, B, Li, Y, Morcos, PA, Doran, TJ, Lu, P and Lu, QL (2009). Octa-guanidine morpholino restores dystrophin expression in cardiac and skeletal muscles and ameliorates pathology in dystrophic mdx mice. *Mol Ther* **17**: 864–871.
20. Wu, B, Moulton, HM, Iverson, PL, Jiang, J, Li, J, Li, J *et al.* (2008). Effective rescue of dystrophin improves cardiac function in dystrophin-deficient mice by a modified morpholino oligomer. *Proc Natl Acad Sci USA* **105**: 14814–14819.
21. Yin, H, Moulton, HM, Betts, C, Seow, Y, Boutilier, J, Iverson, PL *et al.* (2009). A fusion peptide directs enhanced systemic dystrophin exon skipping and functional restoration in dystrophin-deficient mdx mice. *Hum Mol Genet* **18**: 4405–4414.
22. Samoylova, TI and Smith, BF (1999). Elucidation of muscle-binding peptides by phage display screening. *Muscle Nerve* **22**: 460–466.
23. Fletcher, S, Honeyman, K, Fall, AM, Harding, PL, Johnsen, RD, Steinhaus, JP *et al.* (2007). Morpholino oligomer-mediated exon skipping averts the onset of dystrophic pathology in the mdx mouse. *Mol Ther* **15**: 1587–1592.
24. Ahmad, A, Brinson, M, Hodges, BL, Chamberlain, JS and Amalfitano, A (2000). Mdx mice inducibly expressing dystrophin provide insights into the potential of gene therapy for duchenne muscular dystrophy. *Hum Mol Genet* **9**: 2507–2515.
25. Fowler, SC, Zarcone, TJ, Chen, R, Taylor, MD and Wright, DE (2002). Low grip strength, impaired tongue force and hyperactivity induced by overexpression of neurotrophin-3 in mouse skeletal muscle. *Int J Dev Neurosci* **20**: 303–308.
26. Qiao, C, Li, J, Jiang, J, Zhu, X, Wang, B, Li, J *et al.* (2008). Myostatin propeptide gene delivery by adeno-associated virus serotype 8 vectors enhances muscle growth and ameliorates dystrophic phenotypes in mdx mice. *Hum Gene Ther* **19**: 241–254.
27. Glesby, MJ, Rosenmann, E, Nysten, EG and Wroegemann, K (1988). Serum CK, calcium, magnesium, and oxidative phosphorylation in mdx mouse muscular dystrophy. *Muscle Nerve* **11**: 852–856.
28. Wells, DJ, Wells, KE, Walsh, FS, Davies, KE, Goldspink, G, Love, DR *et al.* (1992). Human dystrophin expression corrects the myopathic phenotype in transgenic mdx mice. *Hum Mol Genet* **1**: 35–40.
29. Blake, DJ, Weir, A, Newey, SE and Davies, KE (2002). Function and genetics of dystrophin and dystrophin-related proteins in muscle. *Physiol Rev* **82**: 291–329.
30. Moulton, HM, Fletcher, S, Neuman, BW, McClorey, G, Stein, DA, Abes, S *et al.* (2007). Cell-penetrating peptide-morpholino conjugates alter pre-mRNA splicing of DMD (Duchenne muscular dystrophy) and inhibit murine coronavirus replication in vivo. *Biochem Soc Trans* **35**(Pt 4): 826–828.
31. Tomonari, K (1988). A rat antibody against a structure functionally related to the mouse T-cell receptor/T3 complex. *Immunogenetics* **28**: 455–458.
32. Barclay, CJ, Woledge, RC and Curtin, NA (2009). Effects of UCP3 genotype, temperature and muscle type on energy turnover of resting mouse skeletal muscle. *Pflugers Arch* **457**: 857–864.
33. Lynch, GS, Hinkle, RT and Faulkner, JA (2000). Power output of fast and slow skeletal muscles of mdx (dystrophic) and control mice after clenbuterol treatment. *Exp Physiol* **85**: 295–299.
34. Brooks, SV and Faulkner, JA (1988). Contractile properties of skeletal muscles from young, adult and aged mice. *J Physiol (Lond)* **404**: 71–82.